ELSEVIER

Journal of Magnetism and Magnetic Materials 150 (1995) 13–24

journal of magnetism and magnetic materials

Overview of interlayer exchange theory ☆

J.C. Slonczewski *

IBM Research Division, Thomas J. Watson Research Center, P.O. Box 218, Yorktown Heights, NY 10598, USA

Received 28 November 1994

Abstract

Basic mechanisms of interlayer exchange coupling between two ferromagnets separated by a non-magnetic spacer are surveyed. Simple generic theoretical models yielding closed formulae are treated. First, *intrinsic* exchange between itinerant ferromagnets is treated in the free-electron band approximation, including corrections to the elementary sinusoidal dependences on metallic-spacer thickness and on angle θ included between the magnetic moments. Properties of metallic and insulating spacers are compared. Then three *special* mechanisms of non-cos θ coupling are described: (1) fluctuations of spacer thickness, (2) loose spins, and (3) a novel phenomenological coupling through a non-normal spacer, possibly acting in spacers composed of chromium or manganese.

1. Introduction

Early exchange-coupling studies were made in superlattices composed of RE/Y where RE is one of the magnetic rare earths Gd, Dy, Ho, or Er [1]. The theory, notably by Y. Yafet, was based on the Ruderman–Kittel–Kasuya–Yosida (RKKY) indirect exchange which originally described the coupling between two nuclear spins embedded in a degenerate electron gas. Basic is the effective Hamiltonian

$$H_{\mathrm{eff}}(\rho) = \frac{J_{\mathrm{lc}}^2 m_{\mathrm{e}} Q^4 F(2Q\rho)\mathbf{S}_i \cdot \mathbf{S}_j}{2\pi^3\hbar^2}, \qquad (1)$$

$$F(z) = \frac{z\cos z - \sin z}{z^4},$$

in which the function F is proportional to the nonlocal susceptibility of the gas. Here ρ is the distance between local atomic spins $\mathbf{S}_i$ and $\mathbf{S}_j$, J_{lc} is the exchange integral between a local f-electron and a conduction electron, m_{e} is the electron mass, and Q is the Fermi vector of the free-electron gas. Summing H_{eff} over atomic positions i in one RE magnet and j in the other gives the coupling energy per unit area $W = -J_1 \cos\theta$ where θ is the angle between the two magnetization vectors. This *bilinear* or *Heisenberg* energy expression follows from the factor $\mathbf{S}_i \cdot \mathbf{S}_j$ in Eq. (1) and the linearity of the electron-gas susceptibility.

After the discovery of giant magnetoresistance (GMR) in 1988, the emphasis of exchange studies shifted to ferromagnets of the first transition series, in which the spontaneously spin-polarized electrons have appreciable itinerant character. There exists a comprehensive review of the experimental status of exchange coupling between such ferromagnets separated by metallic spacers [2]. Useful to the interpreta-

☆ This article is based on an invited talk presented at the International Conference on Magnetism 1994, Warsaw, Poland, August 22-26, 1994. The present version was revised January 5, 1995.

* Fax: +1-914-945-4506; email: slon@watson.ibm.com.

SSDI 0304-8853(95)00081-X

tion of experiments is the phenomenological energy series

$$W = -J_1 \cos\theta + J_2 \cos^2\theta + J_3 \cos^3\theta + \cdots, \quad (2)$$

where, by definition, $J_1 > 0$ for 'ferromagnetic' and $J_1 < 0$ for 'antiferromagnetic' coupling. This series describes generalizations of the Heisenberg form of coupling energy.

An excellent current article broadly reviews the theory of exchange coupling through metallic spacers [3]. Here I try to depict succinctly the essential physics, presenting only those theoretical results available as generic closed formulas without specializing to specific electron structures. For discussions of the important topics of 'Fermiology' of oscillatory dependence of exchange on spacer thickness, total-energy computations of exchange, and information about specific multilayer compositions, one must consult reviews [2,3] or the rich original literature.

I first treat *intrinsic* exchange energy in the free-electron band model (Section 2) including non-Heisenberg terms. Then in Section 3 I treat three *special* mechanisms of non-Heisenberg coupling. The first two, considered *extrinsic*, only operate in magnetic multilayers that are either structurally or compositionally non-ideal. The third mechanism is really intrinsic to a spacer made of an abnormal metal manifesting internal exchange forces. I propose a previously unpublished phenomenological coupling expression to describe such multilayers exhibiting what one might call *proximity magnetism*, a concept which could apply to Cr or Mn spacers.

2. Intrinsic exchange

It should be interesting to complement the older RKKY description and emphasize the newer role of itinerant ferromagnetism. For this reason I expose the essential physics by following the resonant-scattering approach of independent works by P. Bruno [4] and M.D. Stiles [5] in the following Subsection 2.1. Their analogy of an optical Fabry–Perot resonator is helpful. It is closely related to the quantum-well concept [6]. Electron transitions observed by inverse photo-emission experiments provide a direct empirical basis for the quantum-well electron states employed in the theory [7]. The resonator

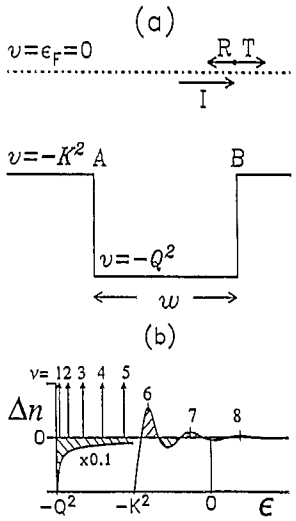

Fig. 1. (a) Potential well for a one-dimensional spinless Fermi gas. (b) Change of density of states Δn due to presence of the well [5]. The bound-state levels marked by vertical arrows, together with transmission resonances marked by the indicated peaks of the continuous part of $\Delta n(\epsilon)$, form one smooth system of sharply defined energy values ϵ_ν ($\nu = 1, 2, 3, \ldots$).

model will serve as background to discussions of anharmonic distortion of coupling oscillations (Subsection 2.2) and a comparison of metallic with insulating spacers (Subsection 2.3).

2.1. Resonator model

To explain in minimal terms the exchange theory, let us first consider *spinless* particles comprising a one-dimensional degenerate Fermi gas overfilling a rectilinear quantum-well potential (Fig. 1a) [5]. Let q be the variable particle wave number and Q the constant Fermi wave number inside the well, and similarly k and K outside the well. The energy $\epsilon = q^2 - Q^2 = k^2 - K^2$ of a Schrödinger particle wave generally propagating through all three subregions of this system is measured from the Fermi potential in reduced units. According to these conventions, the 'crystalline potential' term is $v = -Q^2$ inside the well and $v = -K^2$ outside. The kinetic energy term is respectively q^2 or k^2.

In the range $-Q^2 < \epsilon < -K^2$, there exist a finite number N_b of localized states bound to the well with sharp levels $\epsilon = \epsilon_\nu$ ($\nu = 1, 2, 3, \ldots, N_b$). An incident subwave I with $\epsilon \geq -K^2$ propagating right-

ward within the well scatters from interface B with reflection coefficient $r(\epsilon) = (q-k)/(q+k)$. The reflected part of this wave scatters again at interface A, and so on. For an infinite number of particular discrete values of $\epsilon = \epsilon_\nu$ ($\nu > N_b$), these reflections interfere constructively causing 100% resonant transmission through the spacer of any wave incident from afar. All of these bound-state levels and transmission resonances form a single smooth pattern satisfying the approximate quantum-well relation $qw = q_\nu w = \pi\nu + O(1)$ ($\nu = 1, 2, 3, \ldots, \infty$) where w is the well width. (The exact relation, itself an elementary topic of quantum theory, is not important here.)

Figure 1b shows the change $\Delta n = n(w, \epsilon) - n(0, \epsilon)$ in state density brought about by creation of the well. Upward pointing arrows locate the set of δ-function contributions due to the bound levels. At higher ϵ, the rounded peaks in the dependence of Δn on ϵ mark the transmission resonances. Their widths vary inversely with the dwell time of a resonant particle in the well [5].

The total energy at $T = 0$ K of this one-dimensional solid is the integral of the energy over the occupied states

$$E = \int_{-\infty}^{0} \epsilon n(\epsilon)\, \mathrm{d}\epsilon. \qquad (3)$$

Fig. 2 shows its change $\Delta E = E(w) - E(0)$ versus w. It represents the signed area bounded by $-Q^2 \le \epsilon \le 0$ and lying between the horizontal axis and the curve $n(\epsilon)$ indicated by shading in Fig. 1b, plus the bound-state energy $\Sigma_{N_b}\epsilon_\nu$. According to the above quantum-well relation, one of the resonant peaks of $\Delta n(\epsilon)$, shown in Fig. 1b, passes downward through the Fermi level $\epsilon = 0$ each time w increases by approximately π/Q. Each such passage causes the integral in Eq. (3) to execute an oscillation exhibited in Fig. 2. Approaching the limits $w \to \infty$ and of weak reflections, one finds [5]:

$$\Delta E \to \Delta E_\infty = \left(\hbar^2 Q R^2 / 2\pi m_e w\right) \sin(2Qw). \qquad (4)$$

Here $R = r(\epsilon = 0) = (Q-K)/(Q+K)$ is the reflection coefficient at the Fermi level, and physical units (with m_e = electron mass) are employed. Note that only particle states with ϵ near 0 contribute to ΔE_∞. The dashed curve in Fig. 2 represents this equation, which differs drastically from the exact relation (solid curve) only within the first period of oscillation.

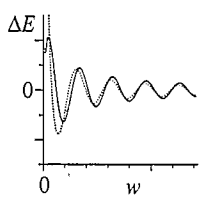

Fig. 2. Total energy versus symmetric-well thickness w for a one-dimensional spinless Fermi gas at $T = 0$ K. The solid curve is exact; the dashed curve is Eq. (4) [5].

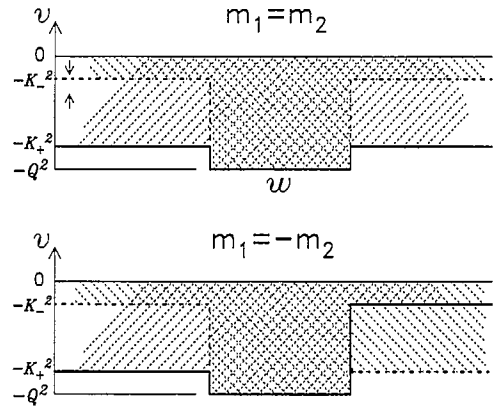

Fig. 3. The four spin-dependent potentials used in calculating the four terms in Eq. (5). The upper two potentials are for parallel ferromagnetic moments, the lower two for antiparallel moments. Different shadings indicate schematically regions occupied by up-spin ↑ and down-spin ↓ electrons.

Turning our attention to the magnetic multilayer, we know that the Stoner exchange potential inside each ferromagnet is spin dependent. Interface reflections differ for majority (+) and minority (−) spin electrons having a given energy ϵ. For reflection coefficients $R_\pm$ at the Fermi level $\epsilon = 0$ we define the difference $\Delta R = R_+ - R_-$. We define a coupling strength $J = [W(\pi) - W(0)]/2$ which usually differs little from J_1. For each of the angles $\theta = 0$ (ferromagnetic moments parallel) and $\theta = \pi$ (antiparallel), the electron wave functions are classed as spin-down ↓ and spin-up ↑. So we write

$$2J = -E_\downarrow(0) - E_\uparrow(0) + E_\downarrow(\pi) + E_\uparrow(\pi) \qquad (5)$$

where $E_{\uparrow \text{ or } \downarrow}(\theta)$ is an integral of type (3) with the subscript ↑ or ↓ attached to $n(\epsilon)$. The potentials for the four terms in this equation are pictured in Fig. 3, showing the two magnet alignments, each with 2

spin directions. We distinguish here the Fermi wave vector $K_{+(-)}$ for majority(minority)-band electrons in the magnets. Note the need for a small extension of the discussion leading to Eq. (4) because the two potential steps are unequal for each of the two antiferromagnetic potentials.

The potential of a three-dimensional trilayer with free-electron bands is invariant with respect to translations parallel to the interfaces. It is energetically equivalent to an aggregate of one-dimensional trilayers, the electrons in each member having the same wave-vector $\mathbf{k}_\parallel$ parallel to the interface. Thus the energy in three dimensions is obtained by integrating the result (5) over the two-dimensional space of $\mathbf{k}_\parallel$. In the limit of weak reflections and large w, the result [4,5] with an inserted temperature factor [4,6] is $J \to J_1$, $J_{n>1} \to 0$ with J_1 of Eq. (2) given by

$$J_1 = (\hbar^2 Q^2/4\pi^2 m_e w^2)(\Delta R)^2 \times \sin(2Qw)(\zeta/\sinh\ \zeta), \qquad (6)$$

where $\zeta = 2\pi k_B T w m_e/\hbar^2 Q$.

The above integration of the one-dimensional behavior of an equation similar to Eq. (4) over the space $\mathbf{k}_\parallel$ mixes different oscillation periods. However, the period π/Q present in Eq. (4) survives asymtotically, because a group of waves with $\mathbf{k}_\parallel$ near 0 gives nearly the same period. Note, however, that Eq. (6) decays more rapidly ($\propto w^{-2}$) than Eq. (4) ($\propto w^{-1}$) because of these interferences. An extension of this consideration gives rise to the spanning-vector construction of the oscillation frequency from the shape of a realistic Fermi surface based on computed band structure of the bulk spacer material [6]. Our specialization to a rectilinear potential for the derivation of Eq. (6) is not necessary, because it is valid for more general potentials providing the reflection coefficients R_+ and R_- are known [4,5]. However, a potential-dependent shift in the phase of the oscillatory dependence of J_1 on spacer thickness occurs.

2.2. Harmonic distortions

When the potential well is deep, the interface reflections are strong and the sinusoidal dependence of $w^2 W$ on w and θ given by Eqs. (2) and (6) become generally distorted [3–6]. One practical way of calculating exchange coupling in the degree of detail needed to show these harmonic distortions is to equate the mutual torque at general θ with the flow of spin angular momentum carried through the spacer by the scattered electrons. This spin-flow method of calculating exchange coupling was first applied to an insulating spacer [8], and later extended to conductors [9].

We define the mean ferromagnetic Fermi vector $\bar{K} = (K_+ + K_-)/2$ and the Fermi-vector ratio $x = \bar{K}/Q$ in the case of a metallic spacer. The spin-flow calculation predicts generally $J_n \neq 0$ for all n and that $w^2 J_1$ has period π/Q in w but is not sinusoidal. In particular, one has at large w, to leading order in $\Delta K \equiv K_+ - K_-$ [10]:

$$J_1 = \frac{\hbar^2 (\Delta K)^2}{4\pi^2 m_e w^2 (1+x^2)(1+x)^2} p(Qw) \qquad (7)$$

where $p(\varphi)$ is a periodic function satisfying $p(\varphi + \pi) = p(\varphi)$. Within the sector $|\varphi| \leq \pi/2$, it can be written as

$$p = \frac{1+x^2}{(1-x)^2}\left\{\varphi - \arctan\left[\frac{1}{2}(x + x^{-1})\tan\varphi\right]\right\} \qquad (8)$$

and is plotted in Fig. 4. Thus Eqs. (7) and (8) separate J_1 into two factors, expressing respectively its envelope, which decays as w^{-2}, and its anharmonic periodicity.

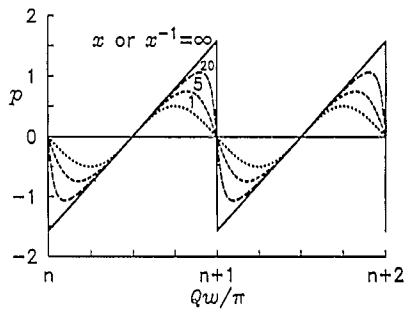

Fig. 4. Periodic factor $p(w)$ ($\propto w^2 J_1$) in the exchange coupling versus spacer width w for four values of the ratio $x = \bar{K}/Q$, according to Eq. (8). The harmonic distortion of exchange coupling grows with the sharpness of transmission resonances as the Fermi vectors of the ferromagnets and spacer are made more different ($x \ll 1$ or $x \gg 1$).

We note the following [10]: Numerical results for $W(w, \theta)$ not relying on the small ΔK approximation agree well with Eqs. (7) and (8) even when the ferromagnetic exchange splitting is as large (2 eV) as calculated ab initio in Fe: $(K_+, K_-) = (1.09, 0.42)$ Å^{-1}. Suppose, moreover, that the non-magnetic spacer also belongs to the first transition series. The trilayer would then be broadly represented by $Q \simeq \bar{K}$. Then $x \simeq 1$, and Eq. (7) predicts $J_1 \simeq (1\ \text{nm}/w)^2 p$ erg cm^{-2}, which is broadly consistent with experiments using Cu spacers [2]. For example, J_1 for bcc(001)Fe/Cu/Fe oscillates with an apparent minimum of -0.6 erg cm^{-2} at $w = 1.4$ nm. Also, for general Q, the function $w^2 J_n(w)$ is predicted to oscillate with n times the frequency of $w^2 J_1(w)$. However, the amplitude of $w^2 J_2$ oscillation amounts to less than 2% of that for $w^2 J_1$. This checks with the analytic expression in our notation

$$J_2 = \hbar^2 (\Delta K)^4 (\sin 4Qw)/2^{12}\pi^2 m_e Q^2 w^2 \qquad (9)$$

derived for the special case $Q = K_-$ [2,8]. Still-higher angular-order terms $w^2 J_n$ are of relative order 10^{-4} or less.

With increasing electron density in the spacer ($x \to 0$) the predicted harmonic distortion of $p(w)$ shown in Fig. 4 increases. In practice this increase is modest; for the fairly extreme case of Fe/Al/Fe, one estimates $x \simeq 0.4$ so that $w^2 J_1(w)$ should fall somewhere between the curve marked $x^{-1} = 5$ and the sinusoid $x = 1$ in Fig. 4.

This predicted increase of harmonic distortion reflects the physical discussion of our one-dimensional solid. Increasing the mean well depth proportional to $Q^2 - \bar{K}^2$ has the effect of strengthening the electron reflection ($R_\pm \to 1$) at the interfaces. The resulting strengthening of multiple reflections sharpens the resonant transmission so that the maxima $\Delta n(\epsilon)$ shown in Fig. 1b become sharper. Thus, whenever varying w causes one of these sharp resonances to pass through the Fermi level, $\Delta E(w)$ calculated according to Eq. (3) develops a quasi-discontinuity in the limit $x^{-1} \to \infty$ which corresponds to one tooth of Fig. 4.

Complementary to our above model, in which both spin-up and spin-down bands are occupied, is the one-band limit ($-K_-^2 \to \infty$) in which the unoccupied spin-up band lies high above the Fermi level. Remarkably, the special case $Q = K_+$ of this limit yields a closed formula for coupling energy at $T = 0$ K [11]. In our notation, its asymptotic form for large Qw is

$$W = \frac{-\hbar^2 Q^2}{8\pi^2 m_e w^2} \sum_{n=1}^{\infty} n^{-3} \sin(2nQw) \cos^{2n}(\theta/2). \qquad (9')$$

Note that each term in this formula having the factor $\cos^{2n}(\theta/2)$ contributes to the first n terms of the series (2), so that here also bivariate harmonic distortion is present.

Eq. (9′) displays an intimate association between the two kinds of harmonic content in the one-band limit. However this association is inverted in our more typical two-band case of finite K_-. Indeed, numerical analysis of this case [10] predicts the harmonic distortion in θ to be *strongest*, with J_2 given by Eq. (9), when reflections and harmonic distortion of $J_n w^2$ with respect to w are *weakest* ($x = 1$).

The above-illustrated contrast in the predicted relative strengths (greater with respect to w than θ) of the two kinds of harmonic distortion of coupling energy deserves comment. Comparison of Eq. (7) with Eq. (9) reveals that the dimensionless expansion parameter for deviations from the Heisenberg-like cos θ coupling is $\Delta K/Q$ (with condition $Q \simeq \bar{K}$). However, the expansion parameter for deviation of $w^2 W$ from sin $2Qw$ behavior expressed by Eq. (8) and shown in Fig. 4 is $x^{-1} = Q/\bar{K}$ because of its origin from transmission resonance. Whereas the values of Q and $\bar{K}$ reflect effects of Coulomb energy, $\Delta K = K_+ - K_-$ measures an internal Stoner-*exchange* energy splitting which is typically an order of magnitude weaker. Therefore a greater harmonic distortion versus w than θ is generally expected.

The presence of $\bar{K}$ or Q in the denominator of these expansion parameters indicates that strong harmonic distortions of both types may be created by design using a spacer or ferromagnets having small pockets in the Fermi surface causing the effective $\bar{K}$ or Q to be small relative to ΔK. The one-band case of Eq. (9′), in which $\Delta K = \infty$, is a case in point. However, we re-emphasize that these *intrinsic* an-

harmonicities are expected to be modest. Experimentally, none with respect to w are reported. Section 3 below makes some references to experimental reports of harmonic distortion with respect to θ (biquadratic coupling).

The dependence of J_1 on well depth predicted by Eq. (7) is substantial. For example, varying Q from $\bar{K}$ to ∞ raises J_1 by the factor 8, according to Eq. (7). A different treatment of the same model interprets, with considerable success, the remarkably systematic experimental variation of exchange coupling versus electron density ($\propto Q^2$) across the Periodic Table [12].

2.3. Metallic versus insulating spacers

Remarkably, P. Bruno recently used a t-matrix technique to derive broadly useful integral expressions for J_n in terms of the reflection coefficients of Bloch waves at the interfaces [4]. They apply to both metallic and insulating spacers. For metals, the w^{-2} dependence of the envelope is asymtotically universal for all terms. For a free-electron metal and large w the leading term for J_1 is Eq. (6) above. For an insulator at $T = 0$ K, Bruno reproduces the previous result

$$J_1(0) = \left\{\hbar^2\kappa^5\left(\kappa^2 - K_+K_-\right)\left(K_+ - K_-\right)^2 \times \left(K_+ + K_-\right)\exp^{-2\kappa w}\right\} \times \left\{2\pi^2 m_e w^2\left(\kappa^2 + K_+^2\right)^2\left(\kappa^2 + K_-^2\right)^2\right\}^{-1} \tag{10}$$

calculated in conjunction with the magnetic-tunneling-valve effect which forms the basis of magnetic STM [8]. Here, κ is the imaginary wave vector and $\nu = \kappa^2$ is the reduced potential in the insulator now lying above the Fermi level. For $T > 0$, one has $J_1(T) = J_1(0)z/\sin z$ where $z = 2\pi k_B T w m_e/\hbar^2\kappa$ [4]. Interestingly, the coupling expressions for metal and insulator spacers are made equivalent by the replacement $Q \to i\kappa$ [4].

According to Eqs. (7) and (10), metallic and insulating spacers behave very differently: For a metallic one, J_1 oscillates versus w; for an insulator, it decays exponentially. For a metallic spacer, J_1 decreases with increasing T but for an insulator J_1 increases with increasing T. Since this growth with T for the insulator is very steep, the coupling is essentially thermally-induced, as observed experimentally using an *amorphous* insulating spacer [13].

3. Special mechanisms of non-Heisenberg coupling

Only one sign of biquadratic coupling $J_2(\geq 0)$ has been reported in all experiments [2]. Since the minima of $\cos^2\theta$ occur at $\theta = \pm\pi/2$, spontaneous orthogonal alignment of sublayer moments is an experimental signature for the dominance of J_2 over J_1. General calculations, such as formulas (9) and (9′) discussed above, however, predict the *intrinsic* $J_n w^2$ through a truly non-magnetic spacer to be very small and/or to oscillate symmetrically about $J_n w^2 = 0$ [3,9,10,11]. The predicted oscillation period of $w^2 J_n(w)$ is simply proportional to $1/n$.

One must therefore appeal to special conditions to explain why the few experiments with measurable J_2 always find $J_2 > 0$. Once such an explanation is in hand, the dominance of biquadratic over the apparent bilinear coupling in some of these experiments might be accounted for by the proximity of experimental w to a node of the intrinsic oscillatory $J_1(w)$ or by cancellation of oscillations of the intrinsic J_1 due to spacer-thickness fluctuations.

Of the three special exchange mechanisms discussed in this section, the first two are extrinsic and $J_2 > 0$ is predicted for all spacer thicknesses. Although the coupling energy predicted by the third mechanism (intrinsic proximity magnetism) is not conveniently expanded in the series (2), it predicts non-colinear ground states with values of θ generally not limited to 0 or π.

3.1. Thickness fluctuations

Our first special mechanism arises phenomenologically from the combined micromagnetic effects of variations of spacer thickness and oscillations of intrinsic J_1 versus w, as known experimentally and represented by Eq. (6) or (7) and (8) [14]. In the structural model of Fig. 5a, the local coupling $J_1(x)$ between the faces of the magnets has the mean $\bar{J}_1$ and steps by amount $\pm 2\Delta J$ at the edges of mono-

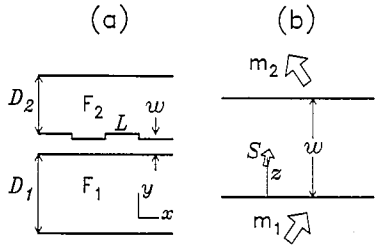

Fig. 5. (a) The thickness-fluctuation model of biquadratic coupling. (b) Loose-spin model of biquadratic coupling.

layer-high terraces having width L. The resulting torque fluctuations induce static spin-wave fluctuations which penetrate exponentially a distance of the order L into each of the ferromagnets. The sum of coupling and exchange-stiffness energies is minimized when the mean moments are orthogonal. Correctly to second order in ΔJ, one has the effective biquadratic coupling

$$J_{2\ \mathrm{eff}} = \left[2L(\Delta J)^2/\pi^3\right] \sum_{i=1,2} A_i^{-1} \coth(\pi D_i/L) \tag{11}$$

where A_i is the exchange stiffness within the ferromagnetic layer of thickness D_i ($i = 1, 2$).

This derivation assumed that L is large compared to the spacer thickness. The sign $J_{2\ \mathrm{eff}} > 0$ comes from the fact that all torques arising from $J_1(x)$ vanish for the special cases of perfect alignment [$\theta(x) = 0$ or π for all x]. For any other uniform orientation of the ferromagnetic moments, the fluctuations of J_1 create torques which are only balanced when the magnets are allowed to relax to a rippled state of varying $\mathbf{m}_1(x, y)$ and $\mathbf{m}_2(x, y)$ having less energy. Ergo orthogonality is favored and therefore $J_{2\ \mathrm{eff}} > 0$. To be precise, it is the *mean* energy that is written $\bar{W} = -\bar{J}_1 \cos\bar{\theta} + J_{2\ \mathrm{eff}} \cos^2\bar{\theta}$ where $\bar{\theta}$ is the angle between the means of the spatially fluctuating $\mathbf{m}_1$ and $\mathbf{m}_2$, and $J_{2\ \mathrm{eff}}$ is given by Eq. (11).

Paradoxically, $J_{2\ \mathrm{eff}}$ *increases* with L or increasing specimen perfection, up to the point that the predicted $J_{2\ \mathrm{eff}}$ becomes as large as ΔJ where the theory breaks down. Numerical energy minimization is then needed [15]. ΔJ and $J_{2\ \mathrm{eff}}$ are as large as 0.40 and 0.10 erg/cm^2 respectively in experiments on bcc (001) trilayers of composition Fe/Cu/Fe [16] in which L ranged between 100 and 200 Å. This is the one experimental system so far interpreted systematically according to this theory. Fluctuations of dipole interactions theoretically contribute to $J_{2\ \mathrm{eff}}$ on the order of 0.01 erg/cm^2 in a micromagnetically similar manner [17]. Thickness-fluctuation mechanisms should create little biquadratic coupling in sputtered multilayers because they effectively have small values of L.

3.2. Loose spins

Eq. (11) predicts only a modest temperature dependence for $J_{2\ \mathrm{eff}}$, owing directly to the temperature dependence of the parameters J_1, A_1, A_2. But in the cases of Al and Au spacers, the experimental J_2 varies by at least two orders of magnitude below room temperature [18,19].

The loose-spin model attempts to account for this strong thermal behavior. It postulates impurities with spin $\mathbf{S}_i$ located inside or at the interfaces of the spacer [20]. The underlying mechanism is fundamentally the strictly Heisenberg-type indirect exchange, described by Eq. (1) in the simplest case, coupling a loose spin to the spins of the ferromagnets. Because it interacts with both magnets, each loose spin contributes to the mutual coupling between them. At high temperatures, the Curie susceptibility of the loose spins is independent of this exchange field and the loose spin contributes only to J_1 via this response. But at lower temperatures this coupling term increasingly departs from the $\cos\theta$ form because the now non-linear loose-spin polarization approaches saturation in the total exchange field acting on it. This non-linearity results generally in $J_n \neq 0$ for all n.

For concreteness, we use the model of Fig. 5b, in which the edges of two ferromagnets having unit magnetization vectors $\mathbf{m}_1$ and $\mathbf{m}_2$ lie at $z = 0$ and $z = w$ respectively. A loose spin with momentum operator $\hbar\mathbf{S}$ lies at position z ($0 \le z \le w$). It is subject to exchange-coupling fields induced by the two ferromagnets through the non-local spin polarizability of the electron gas. The vector sum of these fields, conveniently parametrized according to $\mathbf{U} = U_1(z)\mathbf{m}_1 + U_2(z)\mathbf{m}_2$, gives rise to the effective Hamiltonian $\mathscr{H} = -\mathbf{U}\cdot\mathbf{S}/S$ having the energy levels $\epsilon_m = -Um/S$ with $m = -S, -S+1, \ldots, S$. Here

$$U(\theta) = |\mathbf{U}| = \left(U_1^2 + U_2^2 + 2U_1U_2\cos\theta\right)^{1/2} \tag{12}$$

From conventional statistics, the free energy per loose spin of this level scheme is

$$f(T,\theta) = -k_B T \ln\left(\frac{\sinh\left\{\left[1+(2S)^{-1}\right]U(\theta)/k_B T\right\}}{\sinh\left[U(\theta)/2Sk_B T\right]}\right). \quad (13)$$

Let N be the number of assumedly identical loose spins. We assume conditions such that only J_1 and J_2 are appreciable ($k_B T \gg |U_1| + |U_2|$ or $|U_1| \ll |U_2|$). Then the loose-spin contribution to J_1 is $N[f(\pi) - f(0)]/2$ and the biquadratic coefficient is

$$J_2 = N\left[\tfrac{1}{2}f(0) + \tfrac{1}{2}f(\pi) - f(\pi/2)\right]. \quad (14)$$

One can check this by substituting the first two terms of Eq. (2) plus a constant for $Nf(\theta)$ in this equation.

In the special case $T = 0$ and $|U_1| \ll |U_2|$, the sign $J_2 > 0$ is easy to establish by this argument, similar to the one for thickness fluctuations: To first order, the ground-state quantum-mechanical expectation value $\langle \mathbf{S} \rangle = \pm S\mathbf{m}_2$ has the direction of the field $U_2\mathbf{m}_2$ and the coupling of this one loose spin to $\mathbf{m}_1$ gives the energy $\pm U_1 \cos\theta$, where the sign is the same as that of U_2. This energy is exact for $\theta = 0$ or π. But for any other θ, the energy diminishes when the field $U_1\mathbf{m}_1$ tilts $\langle \mathbf{S} \rangle$ by relaxation away from $U_2\mathbf{m}_2$. The second term of Eq. (2) can only describe energy lowering for $\theta \neq 0$ or π if $J_2 > 0$, which explains the sign of J_2. Further, the energy ϵ_S with Eq. (12) expanded to second order gives the biquadratic coupling at $T = 0$ K as $J_2 = NU_1^2/2|U_2|$ [20,21].

The above theory neglects the scattering effects of loose-spin atoms on the electron waves which communicate bilinear coupling between the ferromagnets. Therefore, it has a better prospect of predicting J_2 than corrections to J_1. Fitting Eqs. (13) and (14) to temperature-dependent data for Fe/Al/Fe [18] gives loose-spin exchange fields in the ranges $|U_1/k_B| \simeq 20$ K, $|U_2/k_B| = 250 - 480$ K [20]. Similar data for Fe/Au/Fe [18,19] yield $|U_1/k_B| = 2.3$ K, and $|U_2/k_B| = 230$ K [20]. These results indicate that the loose spins are probably Fe atoms located very near the interfaces. The small U_1 measures the coupling across, or nearly across the spacer thickness, and the large U_2 measures the coupling to the nearby ferromagnet.

Aside from the Curie temperature of the ferromagnet, we have no ready means of estimating the large loose-spin field U_2. To estimate the small long-range coupling $U_1(z)$, we can take advantage of the bilinearity of the RKKY theory [Eq. (1)] and its predictive equivalent, the resonator model in the limit of weak reflections [Eq. (6)]. For this purpose, we adapt a treatment of the coupling between a semi-infinite ferromagnet and a magnetic monolayer [22]. The coupling U_1 of the first semi-infinite Fe magnet, say, to a loose Fe spin occupying the atomic-volume element ν_a ($= a^3/2$) located at the distance z, is just the *change* in J_1 (with $w \to z$) obtained by adding ν_a to the volume of the second ferromagnet at the spacer-magnet interface. Regarding ν_a as infinitesimal, we have a *differential* rule expressed by $U_1(z) = -\nu_a \mathrm{d}J_1(w \to z)/\mathrm{d}z$.

Application of this differential rule to Eq. (6), which assumes that the ferromagnets are semi-infinite continua, predicts U_1 to be an order of magnitude smaller than our above fit for Al spacers [20]. This inconsistency might be removed if the theory could be extended to take into account the deep potential well implied by the large Fermi vector Q ($\simeq 2.5\bar{K}_{Fe}$) deduced from the valence-electron density of bulk aluminum. We have seen in Eq. (7) that the ferromagnet-ferromagnet coupling increases appreciably with Q because the stronger resonance of a deeper well increases the dwell time of a scattered electron within the well. This fact leads us to conjecture that the long-range ferromagnet–loose-spin coupling $U_1(z)$ should also be increased by a deeper well.

Suppose we now restrict consideration to a homogeneous gas. This might be sensible if the spacer is composed of a transition metal such as copper which should create weaker reflections than aluminum. Then the linearity of the non-local susceptibility in the RKKY theory permits restatement of the differential rule thus: For asymptotically large z, $U_1(z)$ equals $2\nu_a Q$ times $J_1(w \to z)$, but with one quarter of a cycle subtracted from the experimental oscillation of J_1 as a function of spacer thickness w. The differential rule, or its straightforward finite extension to a discrete atomic lattice, may be useful in estimating the loose-spin biquadratic coupling from

measurements of $J_1(w)$ versus w in the absence of loose spins.

Thus the design of such a synthetic loose-spin experiment must take into account that the *maxima* of $|U_1(z)|$, and therefore $J_2(z)$, should occur at distances near the *zeros* of $J_1(w)$ measured in the absence of loose spins. Synthetic loose-spin experiments using fractional magnetic monolayers deliberately deposited within the spacer are currently under way [16,23].

3.3. Proximity magnetism of a spacer

Strictly speaking, Cr and Mn are not 'non-magnetic' spacer elements as often tacitly assumed. The tendency, especially in chromium [24], for bulk antiferromagnetism in the form of incommensurate spontaneous colinear-spin density waves is known. A series of remarkable theoretical papers includes some helicoidal quasi-antiferromagnetic solutions of tight-binding equations in Cr and Mn spacers, even when the ferromagnet moments are externally constrained to be colinear [25]. The prediction $J_2/J_1 = -0.15$ for Fe/Cr/Fe in one of these calculations is remarkably close to certain experimental results discussed below.

The linear polarizability of an elementary nonmagnetic spacer would prevent a helicoidal magnetic state from forming when the ferromagnet moments are colinear. Such a state cannot exist within the framework of our Section 2. This condition inside the spacer, which may be called *proximity magnetism*, arises from the effects of combining a modest internal exchange with a strong exchange coupling across the interfaces to the adjacent ferromagnets [25].

Given the complexity of the unrestricted Hartree–Fock calculations required for the fundamental theory, it may be useful to interpret coupling measurements with the following phenomenological description that reflects the underlying physics. However weak the intra-spacer exchange effects (tending to spontaneous antiferromagnetism or spin-density wave in the bulk) may be, the thermal expectation value $\langle \vec{\sigma}(\mathbf{x}) \rangle$ of the itinerant-electron spin-vector density operator inside the spacer will generally not vanish at temperatures below the Curie point of the ferromagnets. On general grounds of statistical physics, it has no critical temperature of its own, but $\langle \vec{\sigma}(\mathbf{x}) \rangle$ only disappears at the high Curie temperature of the adjoining ferromagnets, each considered as semi-infinite bulk. Hence the term proximity magnetism.

Thinking heuristically in terms of the tight-binding limit, the effective spin of the ith atomic cell within the spacer is the unit-cell integral $\mathbf{S}_i \equiv \int_i d^3 r \langle \vec{\sigma}(\mathbf{x}) \rangle$. Let us assume that all of these atomic-spin vectors lie colinearly in the ground state of our trilayer, as in bulk chromium at low temperatures [24]. (The incommensurate spin-density wave vector of bulk chromium differs by 4% from that of simple alternating antiferromagnetism.) Let us relatively rotate the assumedly uniform ferromagnetic moments $\mathbf{m}_1$ and $\mathbf{m}_2$ away from equilibrium by external means. Consider the relative deviation $\varphi_{ij} (> 0)$ of the atomic-spin *axes* in monolayers i and j from colinear. (Here we do *not* distinguish positive and negative senses of $\mathbf{S}_i$.) The consequent increase of free coupling energy W may be written heuristically $\Sigma_{ij} K_{ij} S_i S_j (1 - \cos \varphi_{ij})$ where K_{ij} is an effective layer–layer exchange integral having either sign. Its values at large separation distances must be significant for the spin-density wave to be incommensurate with the lattice.

Crucial is the assumption that the energetically most important K_{ij} occur at small separations. For nearest neighbors, $\varphi_{i,i+1}$ is small at general θ, except for the very thinnest spacers. In a portion of the generally fluctuating spacer thickness having m monolayers, this deviation is of the order $\varphi_{i,i+1} \simeq \{\theta\}/m$ if the net coupling favors $\mathbf{m}_1 = \mathbf{m}_2$ in the ground state (see Fig. 6a), and $\varphi_{i,i+1} \simeq \{\pi - \theta\}/m$ if it favors $\mathbf{m}_1 = -\mathbf{m}_2$ (see Fig. 6b). Here, the brace notation means that the assigned twist angle $\{x\}$ differs from x by that multiple of 2π which assures $|\{x\}| \leq \pi$.

Thus W is nearly quadratic in φ_{ij}, and therefore in $\{\theta\}$ or $\{\pi - \theta\}$. It is then plausible to write the non-analytic phenomenological formula

$$W = C_+ \{\theta\}^2 + C_- \{\theta - \pi\}^2 \qquad (15)$$

(see Fig. 7) for the *mean* energy, considering the possible fluctuations in spacer thickness. We neglect the possible existence of those *metastable* states which have a twist angle of more than π represented by dashed extensions of the broken curve indicated in Fig. 7. Here the coupling coefficients $C_\pm$ (≥ 0),

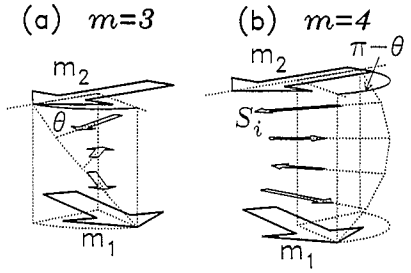

Fig. 6. Illustration of hypothetical twisted quasi-antiferromagnetic proximity states in a spacer of Cr or Mn. The ferromagnetic moments $\mathbf{m}_1$ and $\mathbf{m}_2$ are externally constrained to be non-colinear. In (a), the spacer has an odd number ($m = 3$) of atomic layers; in (b) it has an even number ($m = 4$).

which can only be positive, measure the mean contribution of the portions of the spacer favoring respectively $\mathbf{m}_1 = \pm\mathbf{m}_2$ alignments. Clearly, we assume again that the scale L of thickness fluctuation illustrated in Fig. 5a is large compared to the spacer thickness. However, we must now also assume that L is small enough that exchange stiffness preserves sufficient spatial uniformity of each of the moments $\mathbf{m}_1$ and $\mathbf{m}_2$. By extension of arguments leading to Eq. (11), this condition is

$$L(C_+ + C_-) \sum_{i=1,2} A_i^{-1} \coth(\pi D_i/L) \ll 1, \qquad (16)$$

which is typically satisfied by $L < 100$ Å. Only certain real specimens will satisfy these two bounds on L and therefore obey Eq. (15).

If neither C_+ nor C_- vanishes, the mutual equilibrium orientation of $\mathbf{m}_1$ and $\mathbf{m}_2$ is not colinear ($\theta \neq \pi n$). (Note the general positions of the minima in the example plotted in Fig. 7.) But one or the other of these coefficients $C_\pm$ vanishes if the spacer is perfect (m = constant), and then the equilibrium is colinear ($\mathbf{m}_1 = \pm\mathbf{m}_2$). Comparable mixtures of even and odd m may give $C_+ = C_- > 0$, which constitutes an orthogonal coupling because the minima appearing in Fig. 7 would in this case lie instead at the positions $\theta/\pi = -1/2, 1/2, 3/2 \ldots$.

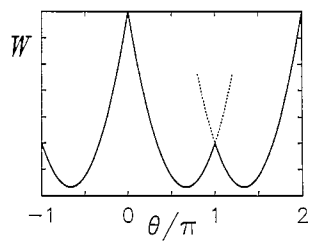

Fig. 7. A hypothetical example of the exchange energy (15) for a trilayer with proximity magnetism in the spacer having thickness fluctuations. Antiparallel coupling predominates in the plotted example: $W = C(\{\theta\}^2 + 2\{\pi - \theta\}^2)$. The dashed curve segments represent metastable conditions.

A crucial difference between Eq. (15) and any finite sum having the form of Eq. (2) is that the *saturation* torque $dW/d\theta$ for the orientation $\mathbf{m}_1 = \mathbf{m}_2$ ($\theta = 0$) vanishes in the latter but has two values $\pm 2\pi C_-$ in the former. Here, the $\pm$ sign depends on the sense of micromagnetic twist through the spacer portions of antiparallel coupling (assumed all alike). Operationally, this sign depends on whether the condition $\theta = 0$ is approached from below ($\theta < 0$) or above ($\theta > 0$). Thus, whereas Eq. (2) implies full saturation of the M–H curve at a finite critical external field $H = H_c$, Eq. (15) implies *asymptotic approach toward saturation*. The latter saturation is not complete for any finite field because the torque $\pm 2\pi C_- \neq 0$ precludes the possibility of a minimum, even though the total energy is symmetric about $\theta = 0$.

Parenthetically, we comment that the same behavior is predicted under similar structural conditions if the spacer is an ordinary alternating-spin antiferromagnet. In addition, we may consider bridges filled with ferromagnetic material passing through an imperfect non-magnetic spacer. The mean energy of such bridges, also known as *pinholes*, should theoretically obey Eq. (15) with $C_- = 0$ and $C_+ > 0$. This fact is apparent from the derivation of the quasi-parabolic exchange energy of conical bridges illustrated in Fig. 6 of Ref. [27].

The very many coupling measurements with chromium (001) spacers have been interpreted using the first two terms of Eq. (2) as if chromium were a normal simple metal [2]. However, we argue that some of the data is better understood in terms of our proximity-magnetism phenomenology which attempts to reflect results of n-electron quantum theory [25]:

(1) The Kerr-effect magnetization loops of Fe/Cr/Fe sometimes approach saturation gradually [26].

(2) Spin-polarized neutron reflection data for a Fe/Cr superlattice shows periodically alternating

transverse components of ferromagnetic sublayer moments which only align gradually in up to several kilogauss of increasing external field [28].

(3) The *apparent* J_2 measured by means of the Kerr effect varies as w^{-1} for large w [26]. Intrinsic coupling predicts w^{-2} behavior for the envelope of J_n (Section 2), and imperfections of structure only make it fall faster. But a w^{-1} or m^{-1} dependence of $C_{\pm}$ follows naturally from our above discussion [$W \propto mK_{ij}(\theta/m)^2 \propto m^{-1}$].

(4) Compelling is the fact that very differently prepared and measured Fe/Cr/Fe specimens – (GaAs substrate and M–H loops [29]) versus (Fe whisker and Brillouin light scattering [2]) – have one property in common: $J_1/J_2 \simeq -3$ for several values of mean m in the first negative lobe of long-period coupling ($3 \leq m \leq 13$). This ratio J_1/J_2 is nearly constant even though J_1 and J_2 oscillate strongly with the $\simeq 2$ monolayer short period in the whisker-based sample, yet not in the GaAs-based sample. Surely this structurally invariant ratio must be *intrinsic* to ideal epi Fe/Cr/Fe trilayers having spacer thicknesses in this range!

To explain the reason for this constant characteristic ratio, let us embrace the experimental evidence that the long-period coupling generally (but not completely) dominates the short-period coupling throughout this first negative lobe of the long-period coupling. Then ideally we have $C_+(m) = 0$ for most values of m in this range $3 \leq m \leq 13$, and perhaps $C_+(m)$ is small for certain ones ($m = 3$, 11, 13) [2]. The mean coupling of any real spacer whose thickness fluctuates within this range should therefore typically satisfy $C_+ \ll C_-$. The observed coupling oscillations imply that, depending on character of the sample, the mean C_- (> 0) versus the mean m oscillates with the short period (but without sign change).

Suppose we crudely represent Eq. (15) with the technically inapplicable first two terms of Eq. (2) by setting the difference between these expressions to a constant at the three representative orientations $\theta = 0$, $\pi/2$, and π. We then find that Eq. (15) effectively predicts $J_1 \simeq -\pi^2 C_-/2$ and $J_1/J_2 \simeq -2$ if we neglect C_+. Since the predicted ratio -2 is not far from the experimental $\simeq -3$, our interpretation in terms of proximity magnetism using one adjustable parameter C_- is more economical than the conventional one using two parameters J_1, J_2. A proper test of proximity-magnetism phenomenology would require the direct employment of Eq. (15) instead of Eq. (2) in deriving the M–H loops, Brillouin-scattering frequencies, neutron-reflection intensities, etc. for comparison with experiments.

Acknowledgements

Heartfelt thanks are due to P. Grünberg, Q. Leng, M. Schäfer, B. Heinrich, J. Cochran, A. Arrott, A. Schreyer, G. Prinz, M. Filipkowski, J. Krebs, and D. Edwards for stimulating discussions and access to their research results prior to publication.

References

[1] C.F. Majkrzak et al., Adv. in Phys. 40 (1991) 99.
[2] B. Heinrich and J.F. Cochran, Adv. in Phys. 42 (1993) 523.
[3] K.B. Hathaway, in: Ultrathin Magnetic Structures, eds. B. Heinrich and A. Bland (Springer, Berlin, 1994), p. 45.
[4] P. Bruno, J. Magn. Magn. Mater. 121 (1993) 248; Europhys. Lett. 23 (1993) 615; Phys. Rev. B 49 (1994) 13231.
[5] M.D. Stiles, Phys. Rev. B 48 (1993) 7238.
[6] D.M. Edwards, J. Mathon, R.B. Muniz and M.S. Phan, J. Phys. Cond. Matt 3 (1991) 4941; Phys. Rev. Lett. 67 (1991) 493, 1476; J. Mathon, M. Villeret and D.M. Edwards, J. Phys. Cond. Matt. 4 (1992) 9873.
[7] J.E. Ortega, F.J. Himpsel, G.J. Mankey and R.F. Willis, J. Appl. Phys. 73 (1993) 5771; and references therein.
[8] J.C. Slonczewski, Phys. Rev. B 39 (1989) 6995.
[9] K.B. Hathaway and J.R. Cullen, J. Magn. Magn. Mater. 104–107 (1992) 1840; R.P. Erickson, K.B. Hathaway and J.R. Cullen, Phys. Rev. B 47 (1993) 2626.
[10] J.C. Slonczewski, J. Magn. Magn. Mater. 126 (1993) 374.
[11] D.M. Edwards, J.M. Ward and J. Mathon, J. Magn. Magn. Mater. 126 (1993) 380.
[12] E. Bruno and B.L. Gyorffy, Phys. Rev. Lett. 71 (1993) 181.
[13] B. Briner and M. Landolt, Europhys. Lett. 28 (1994) 65.
[14] J.C. Slonczewski, Phys. Rev. Lett. 67 (1991) 3172.
[15] R. Ribas and B. Dieny, J. Magn. Magn. Mater. 121 (1993) 313.
[16] B. Heinrich, Z. Celinski, J.F. Cochran, A.S. Arrott, K. Myrtle and S.T. Purcell, Phys. Rev. B 47 (1993) 5077.
[17] S. Demokritov, E. Tsymbal, P. Grünberg and W. Zinn, Phys. Rev. B 49 (1994) 720.
[18] C.J. Gutierrez, J.J. Krebs, M.E. Filipkowski and G.A. Prinz, J. Magn. Magn. Mater. 116 (1992) L305.
[19] A. Fuss, J.A. Wolf and P.A. Grünberg, Physica Scripta T45 (1992) 95.
[20] J.C. Slonczewski, J. Appl. Phys. 73 (1993) 5957.

[21] J. Barnaś and P.A. Grünberg, J. Magn. Magn. Mater. 121 (1993) 326.
[22] W. Baltensperger and J.S. Helman, Appl. Phys. Lett. 57 (1990) 2954.
[23] P. Grünberg and M. Schäfer, private communication.
[24] E. Fawcett, Rev. Mod. Phys. 60 (1988) 209.
[25] D. Stoeffler and F. Gautier, Prog. Theor. Phys. Suppl. 101 (1990) 139; J. Magn. Magn. Mater. 121 (1993) 259.
[26] Q. Leng, private communication.
[27] O. Massenet, F. Biragnet, H. Juretschke, R. Montmory and A. Yelon, IEEE Trans. Magn. 2 (1966) 553.
[28] A. Schreyer, J.F. Ankner, Th. Zeidler, M. Schäfer, H. Zabel, C.F. Majkrzak and P. Grünberg, private communication.
[29] U. Köbler, K. Wagner, R. Wiechers, A. Fuß and W. Zinn, J. Magn. Magn. Mater. 103 (1992) 236.